32nd CERES Science Team Meeting 2019, Oct 29–31, Lawrence Berkeley National Laboratory, Berkeley, CA, USA

Examining Cloud Changes over the Eastern Pacific Using CALIPSO and CloudSat

Seung-Hee Ham[1], Seiji Kato[2], Fred Rose[1], Kuan-Man Xu[2], and Tyler Thorsen[2]

[1]Science Systems and Applications, Inc. (SSAI), Hampton, Virginia, USA
[2]NASA Langley Research Center, Hampton, Virginia, USA

Motivation

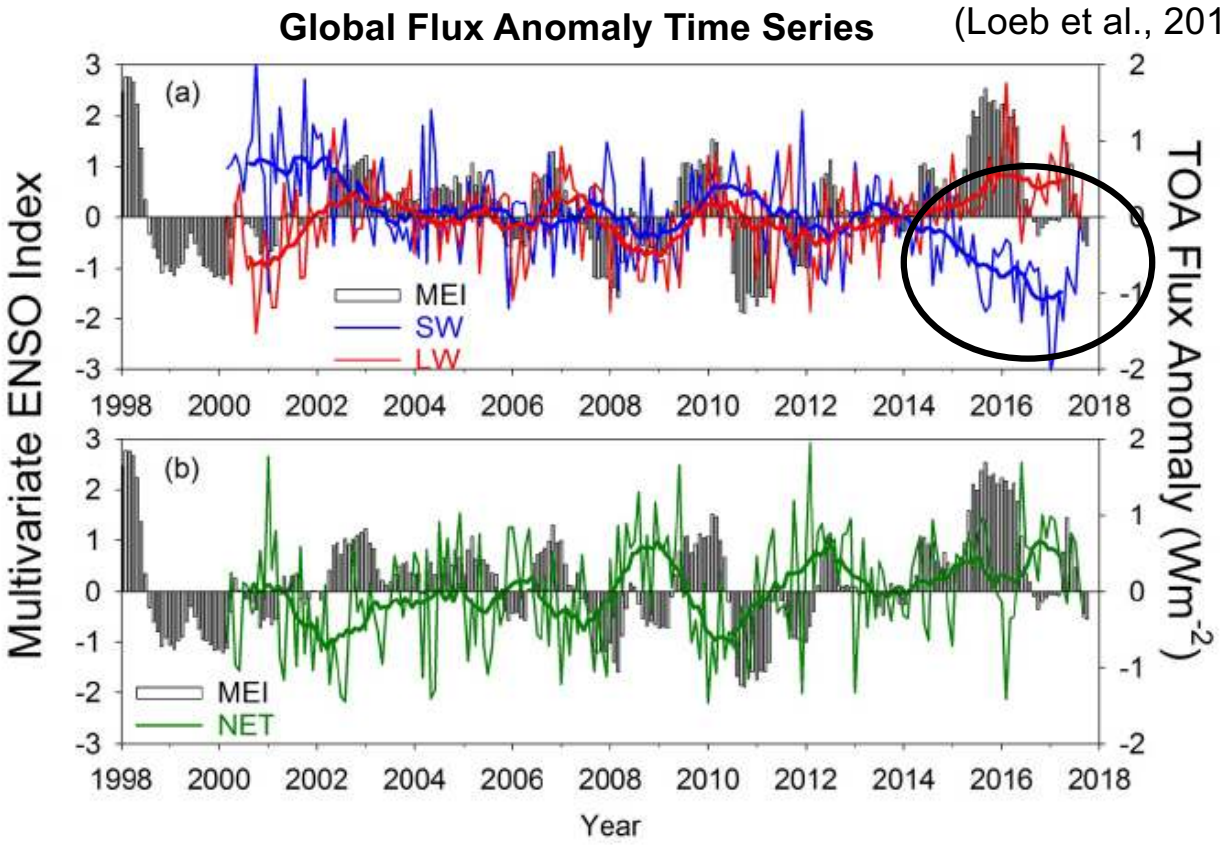

Thin lines: monthly anomalies

Thick lines: 12 month running means of anomalies

- Large negative outgoing SW anomaly has been observed since 2014, and the negative anomaly lasted until the end of 2017.
- The negative outgoing SW anomaly caused net warming of Earth.

Motivation

- Hiatus Period: July 2000 – June2014
- Post-Hiatus Period: July 2014 – Sep 2017

(Loeb et al., 2018)

SW Changes between the two periods contributed by Low Clouds

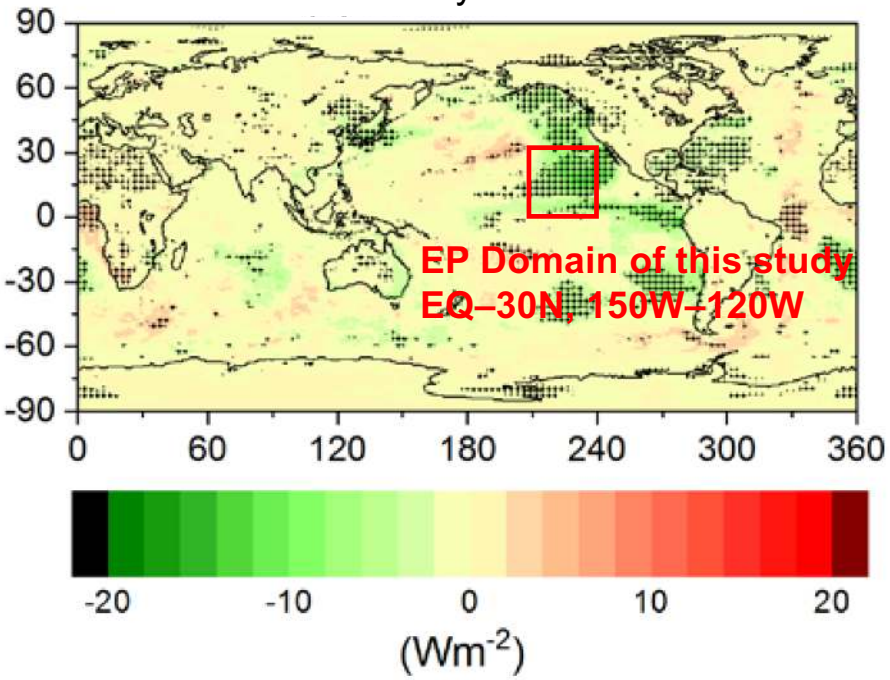

SW Changes between the two periods contributed by Mid+Hi Clouds

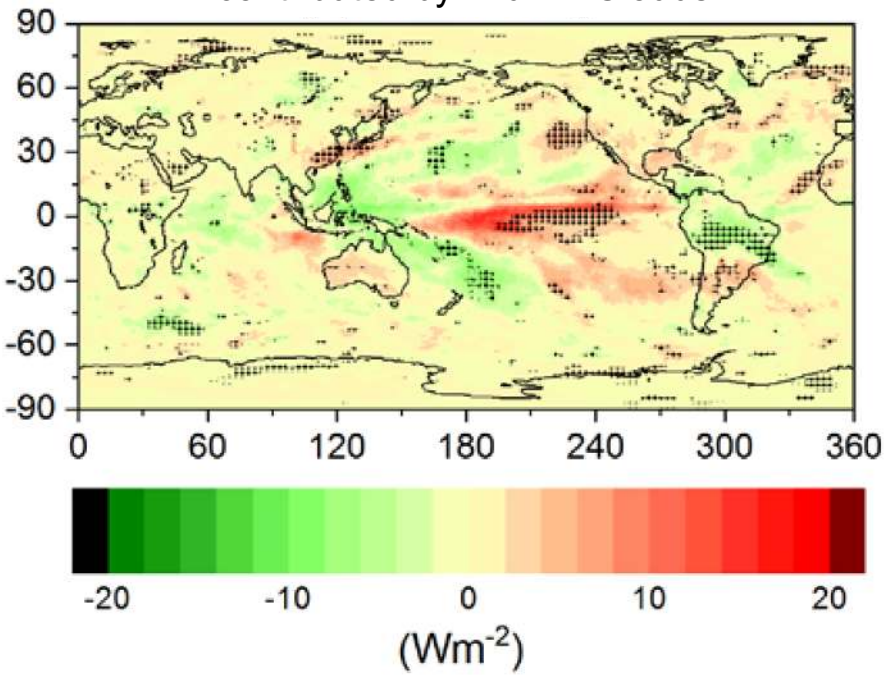

- The strong negative SW anomaly is largely contributed from a reduction of low-level clouds over the North Eastern Pacific.

Objectives

- Examine detailed vertical cloud changes over the Eastern Pacific using CALIPSO and CloudSat observations
- Examine if there are significant/noticeable differences in cloud properties when using active sensors, as oppose to passive sensors
- Relate the cloud changes to meteorological conditions using MERRA-2 reanalysis dataset

Datasets

- ❑ MODIS (Passive sensor) cloud properties: CERES Ed4A SSF Aqua hourly data
- ❑ CALIPSO (Lidar) cloud properties: CALIPSO V4 VFM product
- ❑ CloudSat (Radar) cloud properties: CloudSat R05 2B-GEOPROF, 2B-CWC-RO
- ❑ CloudSat + CALIPSO (Radar+Lidar) cloud properties:

  Combination of CloudSat R05 and CALIPSO V4 based on Kato et al. (2010)
- ❑ CERES EBAF Ed4.1 flux dataset
- ❑ Meteorological properties: MERRA-2

  Sea surface temperature (SST), temperature, humidity, and vertical velocity

- *CloudSat has been operating for daytime only since June 2012, and for the consistency, cloud properties for daytime are analyzed for all cloud datasets. Also we use MODIS SSF Aqua for consistent sampling with CloudSat and CALIPSO, since all of are in A-train.*

Cloud Boundaries from CALIPSO V4 and CloudSat R05

- The main concept is based on Kato et al. (2010): CALIPSO (CALIOP) provides cloud boundaries at a finder vertical resolution (30 m or 60 m) than CloudSat (CPR) (480 m but oversampled every 240 m), and thus we keep the CALIOP cloud boundary if the CALIPSO signal is available. When clouds are thick and the CALIOP signal is fully attenuated, we use CloudSat CPR to assign clouds below the CALIPSO attenuation level.
- **Definition of CALIPSO clouds**

  According to CALIPSO V4 VFM product, we select cloud features with a high confidence (CAD score > 70). For liquid clouds < 4 km, clouds from single-shot (333 m) beam are only used. For ice phase, clouds from all scales of horizontal spatial averaging (333-m, 1, 5, 20, and 80 km) are used.
- **Definition of CloudSat clouds**

  Cloud mask value ≥ 30 from 2B-GEOPROF product (0: completely clear, 40: completely cloudy). It seems that most of surface clutters are assigned as 5.

CALIPSO Only

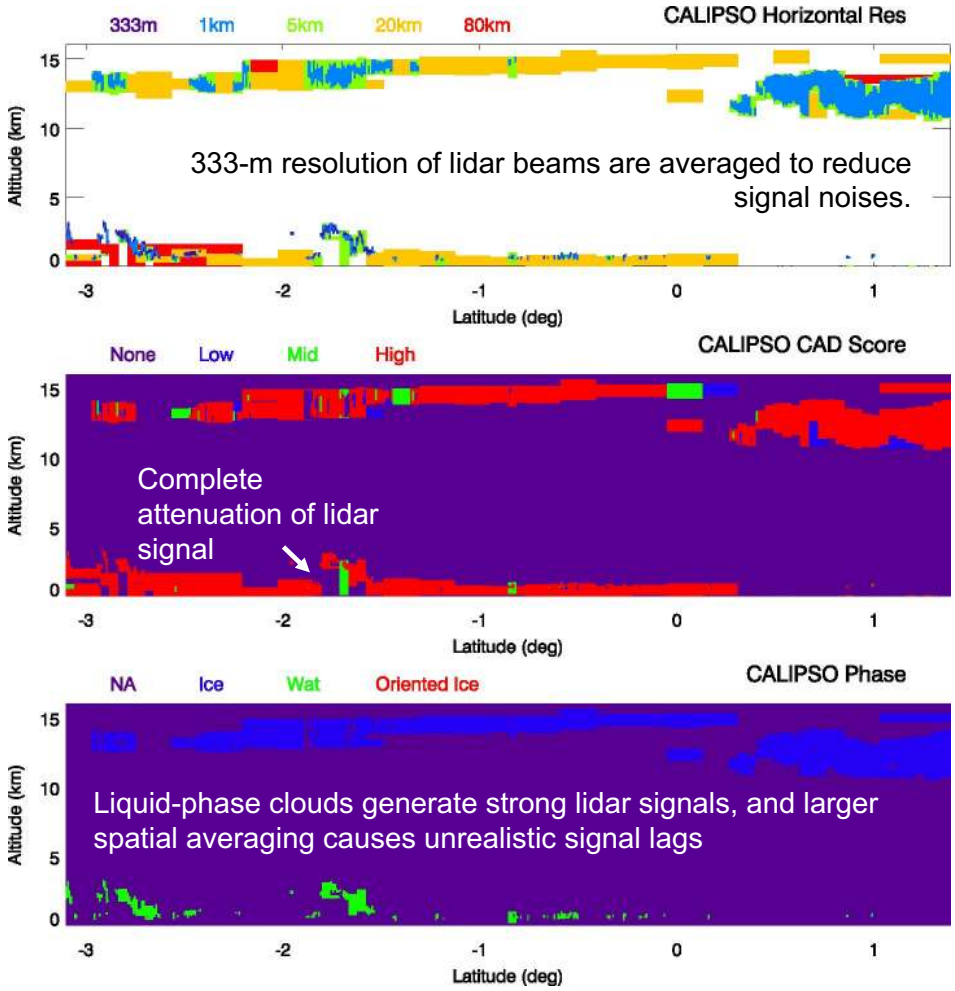

1 July 2008 01:54UTC Track

CloudSat Only

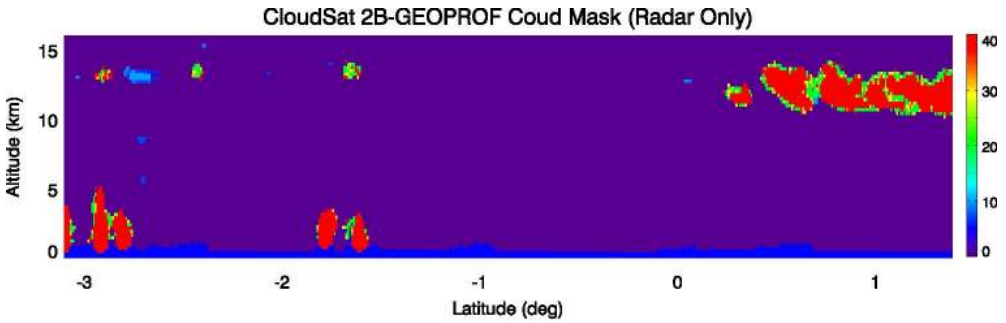

CALIPSO + CloudSat

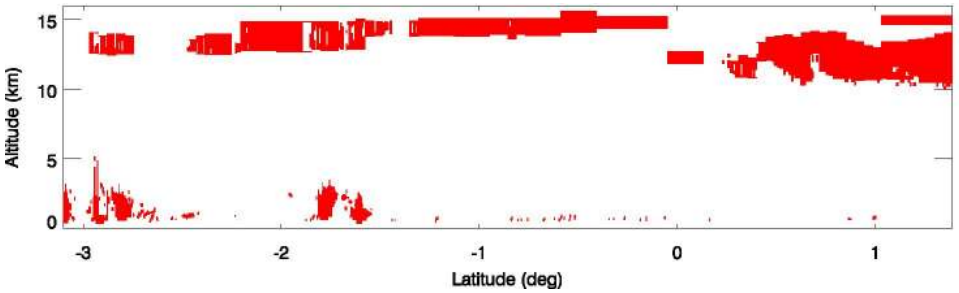

- High-level clouds are well captured by CALIPSO (probably too sensitive to very thin clouds).
- CloudSat sees a thick cloud layer through the cloud base, but the CALIPSO signal is fully attenuated.
- CALISPO captures small-scale boundary layer clouds, but CloudSat does not.

Cloud Volume Fraction Profile (%)

- 125 reference vertical layers are defined with a constant depth of 160 m from 0 km to 20 km. Then the cloud volume profile (%) is computed as the fraction of volume filled by clouds within each vertical bin.

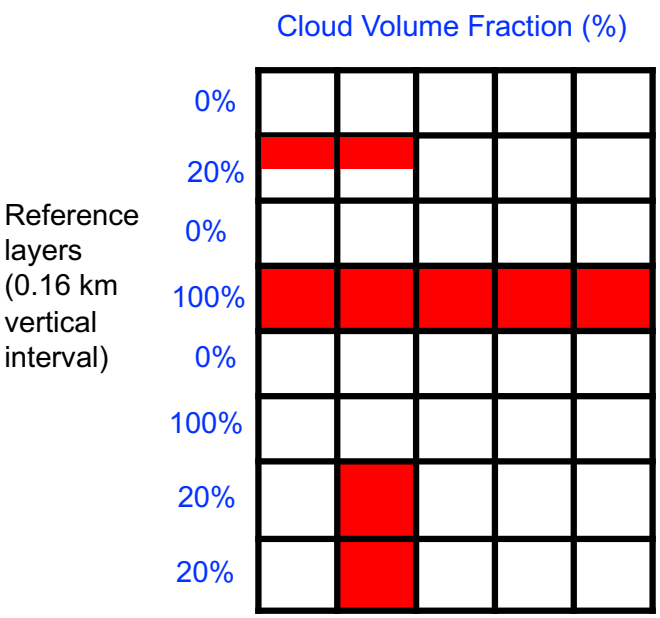

Cloud Cover (%) (Traditionally used)

- For the assigned altitude range (e.g., 0-3 km for low clouds, >10 km for high clouds), cloud-occupied area from satellite view is computed.

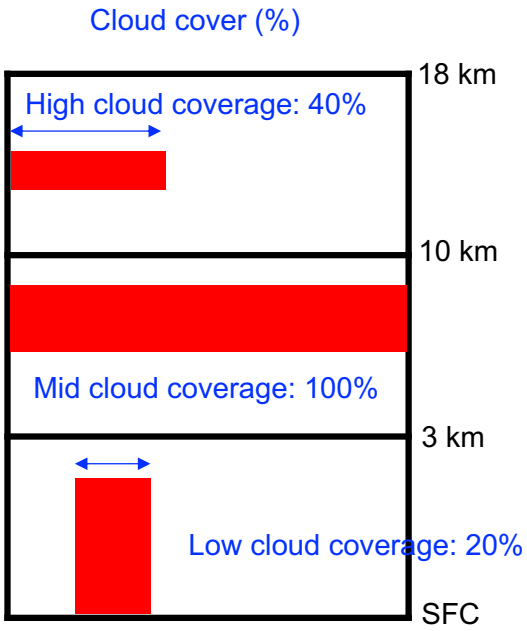

Cloud Volume Fractions (%) over the Eastern Pacific (EP) (150W-120W, EQ-30N)

MODIS

The cloud top variability of high-level clouds is smaller compared to CALIPSO and CloudSat.

CloudSat

CloudSat misses small-scale cumulus clouds and thin cirrus clouds. Cloud volumes are underestimated for high and low-level clouds.

CALIPSO+CloudSat (CC)

Cloud top variability of high-level clouds is largest. Low-level clouds amount is also largest among the datasets.

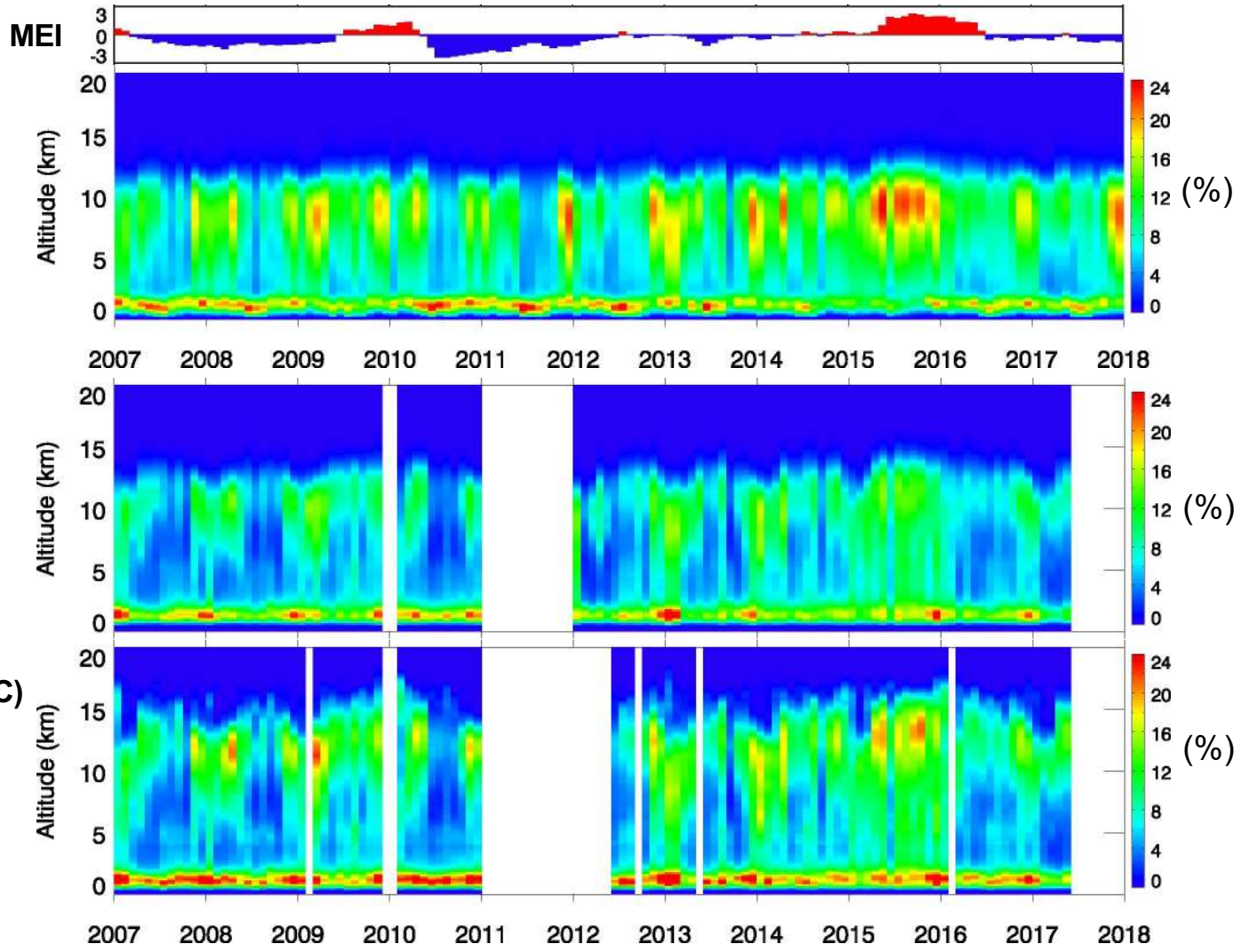

Cloud Volume Fraction (%) Anomalies over the EP (150W-120W, EQ-30N)

MODIS
Larger negative anomaly of low-level clouds during 2015/16 El Niño compared to other datasets

CloudSat
Similar to CALIPSO except very low clouds

CC
CloudSat/CloudSat indicates a decrease of low-level clouds in the beginning of 2015 and 2017.

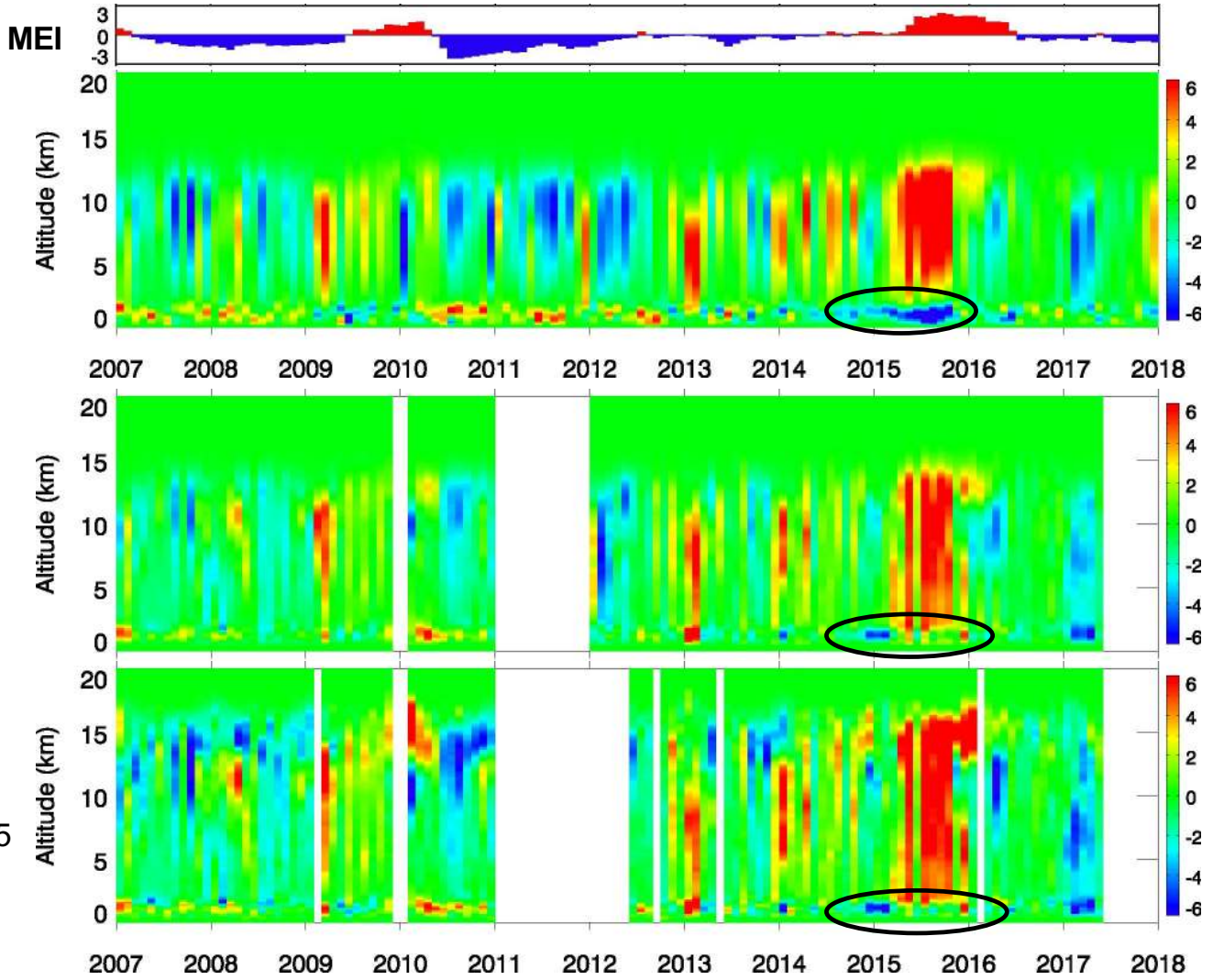

The differences in low cloud anomalies from MODIS and CC during 2015/16 El Niño might be related

1) Uncertainty of MODIS sensor for multi-layer clouds
2) Full attenuation of CALIPSO signal and limitation of CloudSat near surface.

Cloud Cover (%) Anomalies over the EP (150W-120W, EQ-30N)

Smoothed with a 3-month moving window

MODIS

CC

SST (K)

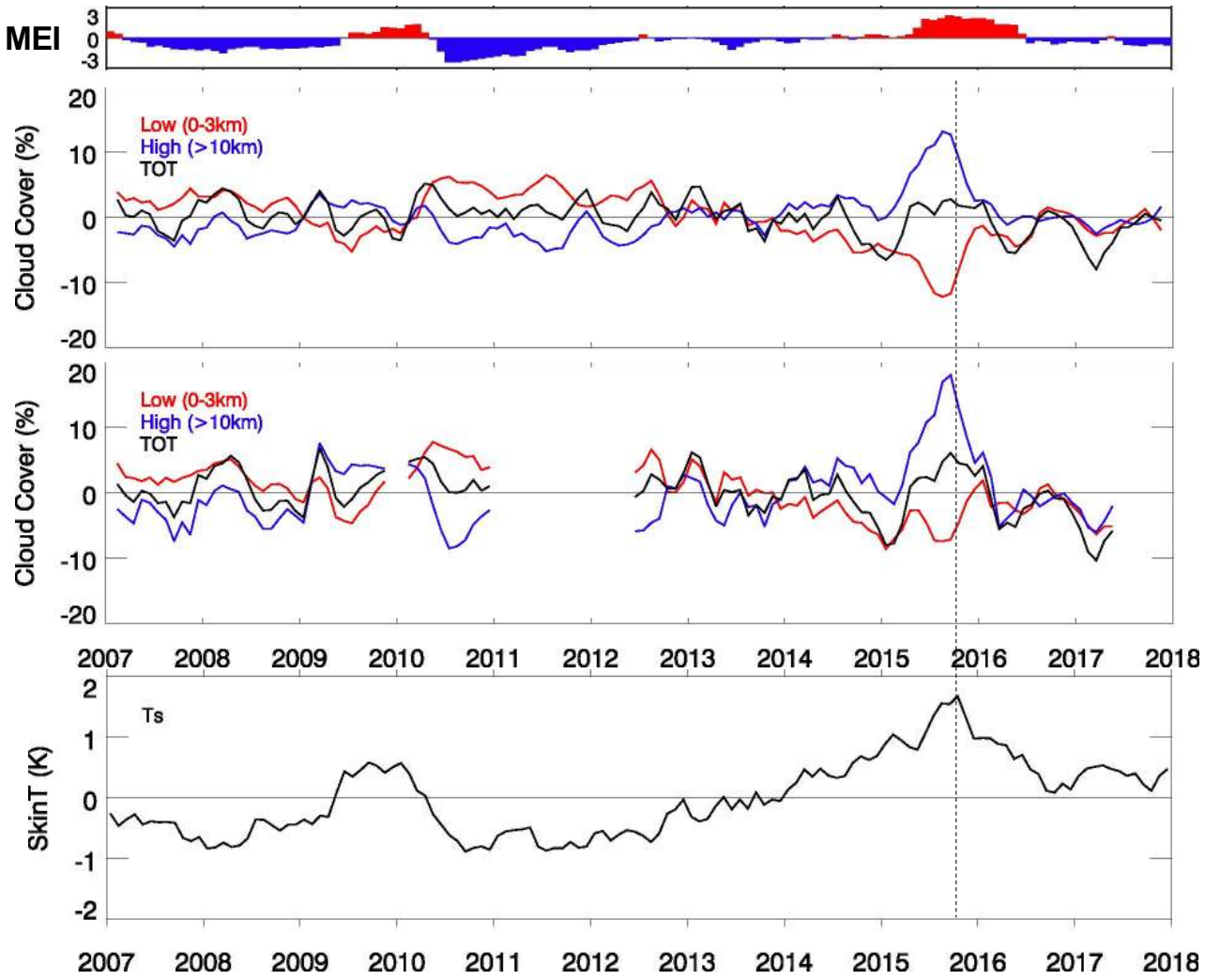

- CC shows slightly larger high-level cloud anomalies and smaller low-level cloud anomalies during 2015/16 El Niño.
- Since 2016, total cloud cover reduced in MODIS and CC, explaining why the strong negative SW anomalies occurred.
- The reason for high-level cloud reduction in 2016 is due to decreased vertical motion and RH (next slide), and the reason for low-level decrease is lingered warm SST anomalies and weakened inversion of boundary layer (next slide).

Meteorological conditions over the EP (150W-120W, EQ-30N)

- During El Niño seasons (e.g., the end of 2009 and 2015), positive anomalies in SST, low-troposphere specific humidity, and upward vertical motion occur.
- After positive anomalies of SST, mid/upper troposphere (5-13 km) air temperature increased and tropopause temperature (13-18 km) decreased in the following spring.
- As a result, relative humidity decreased at 5-13 km, and increased at 13-18 km in the next spring of El Niño.

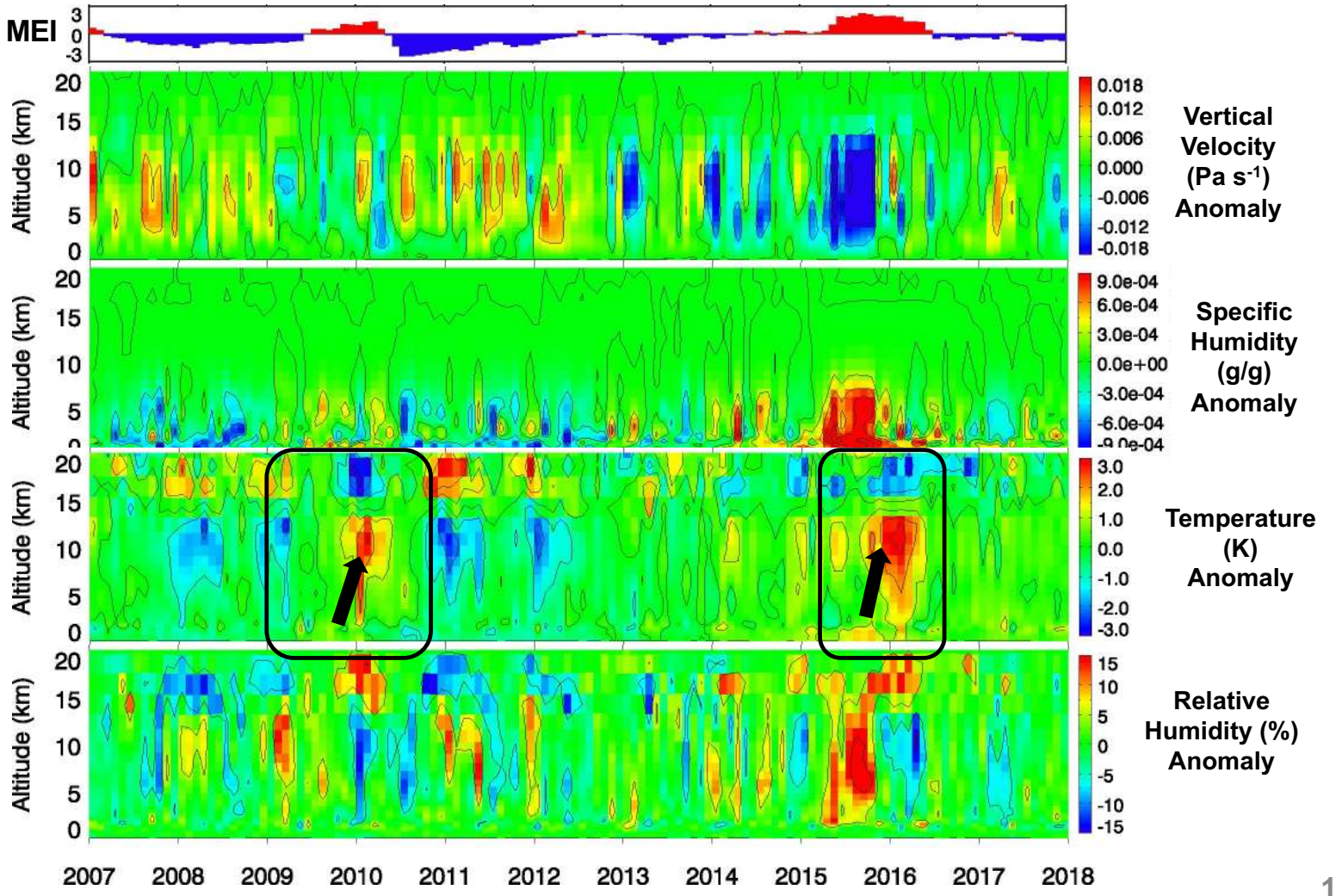

RH (%) versus Cloud Volume Fraction (%) Anomalies over the EP (150W-120W, EQ-30N)

Relative Humidity (%) Anomalies

CC Cloud Volume (%) Anomalies

MODIS Cloud Volume (%) Anomalies

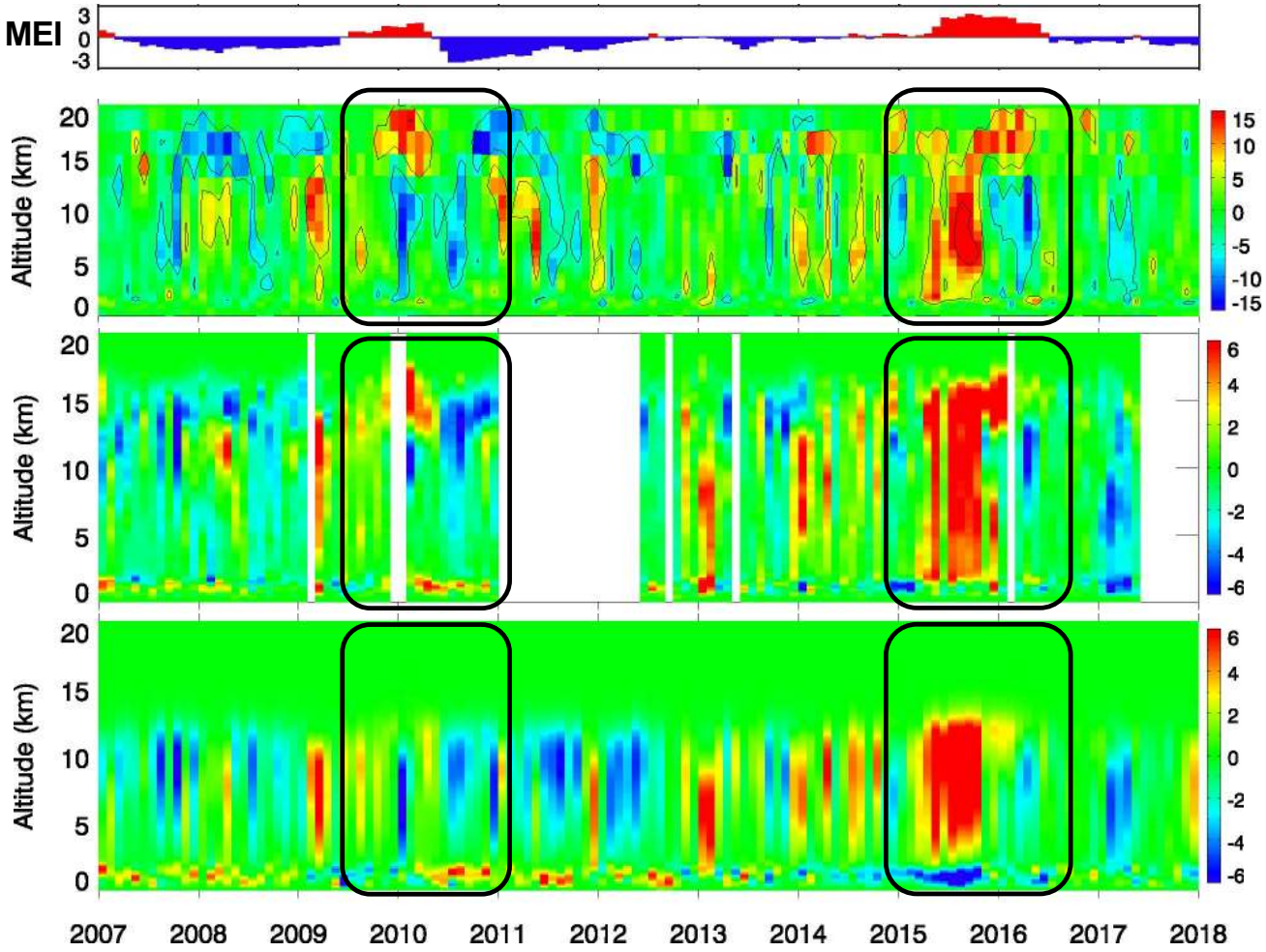

- Anomaly patterns of relative humidity (%) are well agreed with cloud volume anomalies.
- Particularly in the upper troposphere, CC merged cloud volume anomalies are better agreed with RH anomalies, compared to MODIS cloud volume anomalies.

Cloud Top Height over the Eastern Pacific (EP) (150W-120W, EQ-30N)

- While cloud cover anomalies happen coincidently with SST anomalies, the increase of cloud top boundary of high-level clouds lags behind of SST positive anomalies.
- An increase of low-level cloud top precedes Ts peaks.

Smoothed with a 3-month moving window

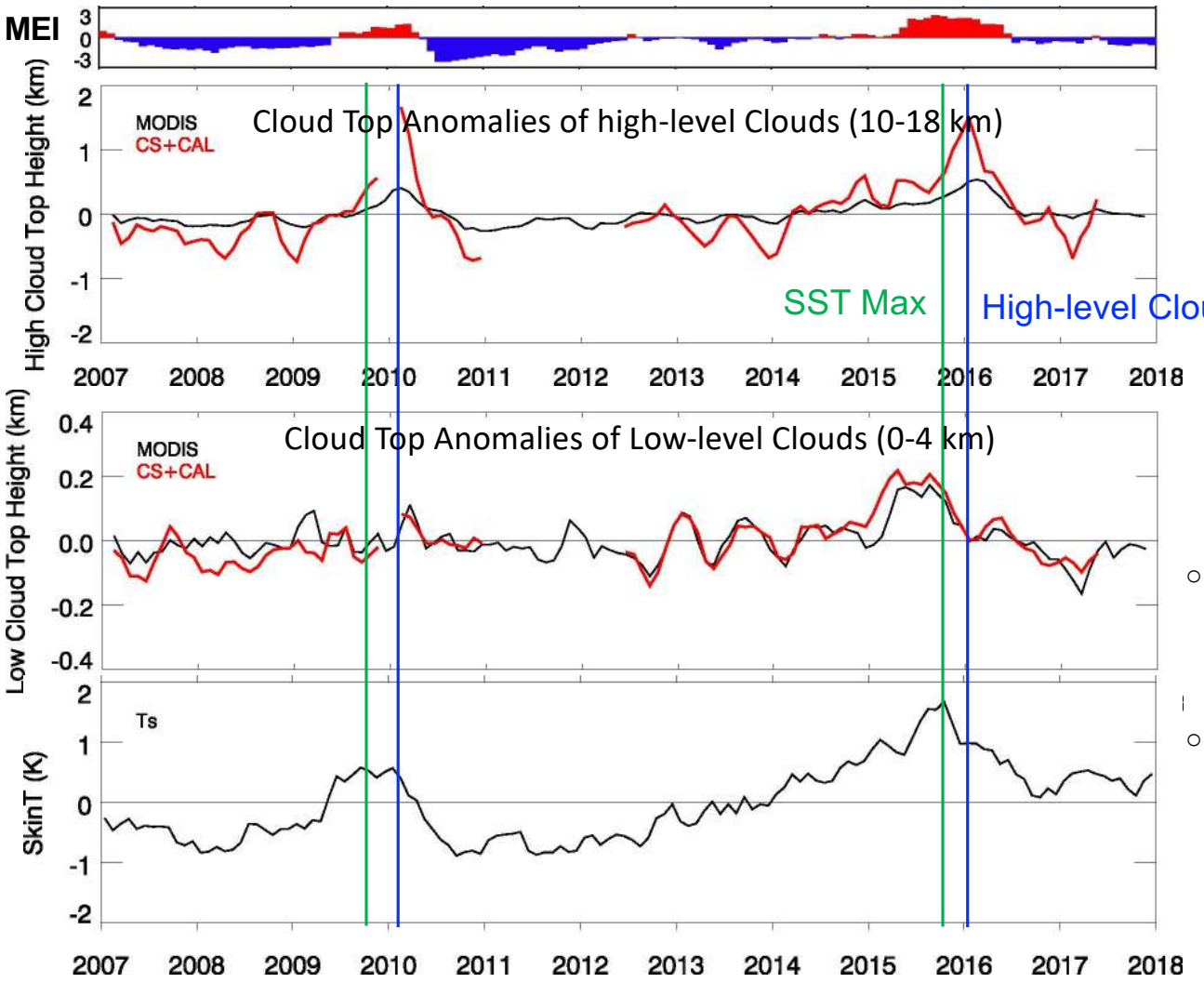

- *Cloud top boundary of high-level clouds is defined between 10-18 km.*
- *Cloud top boundary of low-level clouds is defined between 0 and 4 km.*

Relationships between RH (%) and Cloud Volume Fraction (%) over the EP

# of Cases based on MERRA-2 RH

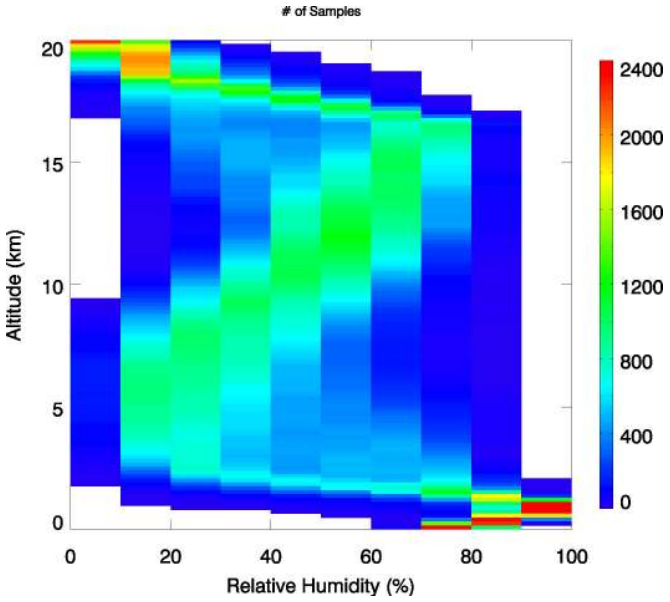

CC Cloud Volume Fraction (%)

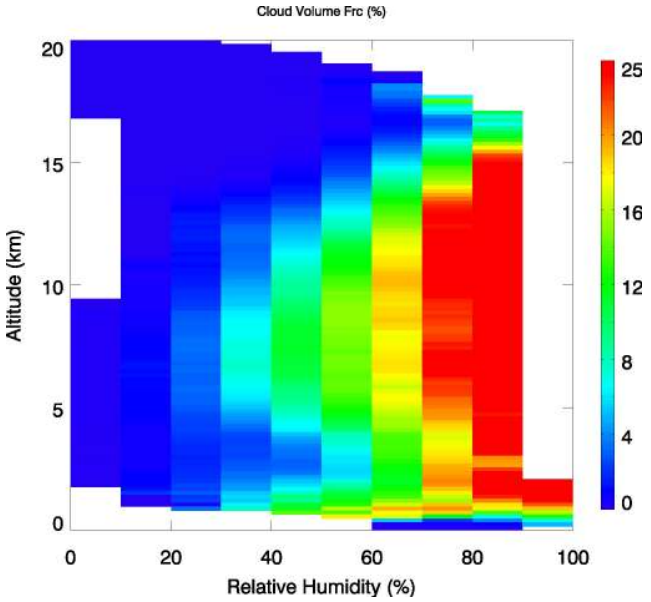

MODIS Cloud Volume Fraction (%)

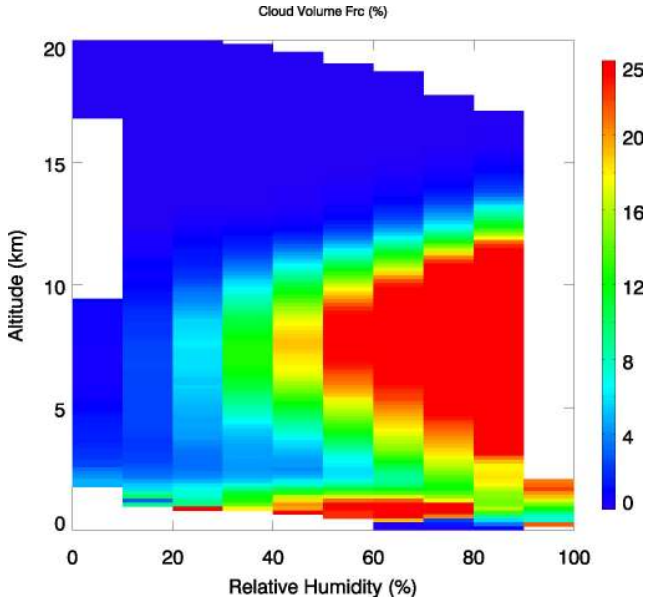

5° gridded monthly profiles for 2007–2017 over the EP are used for the statistics.

Summary and Conclusions

- Merged cloud boundaries from CALIPSO and CloudSat (CC) are consistent with those from MODIS, except for high-level clouds. CC clouds show a larger variability of high-level cloud tops depending on ENSO events, in comparison to MODIS cloud tops.
- In 2016, all-levels of cloud amounts decreased, resulting in large negative SW anomalies. The sudden decrease of cloud amounts is related to reduced vertical motion and lingered warm SST over the EP.
- Mid troposphere warmed up and tropopause temperature cooled down 2-3 months later after SST warmed during El Nino events due to latent heating. This further causes decrease of relative humidity in mid troposphere, and increase of relative humidity in upper troposphere. As a result, high-level cloud top boundary elevated 2-3 months after SST peaks. This feature is better captured in CC measurements, compared to MODIS.

Back Up

Cloud Extinction Profiles over EP (150W-120W, EQ-30N)

MODIS Extinction Coeff k_{ext} (km^{-1})

CloudSat Extinction Coeff k_{ext} (km^{-1})

CloudSat Water Content ($mg\ m^{-3}$)
Liquid and ice phase algorithms separately run in CloudSat. Cloud particle has a significant impact on CWC ($Z \propto D^6$).

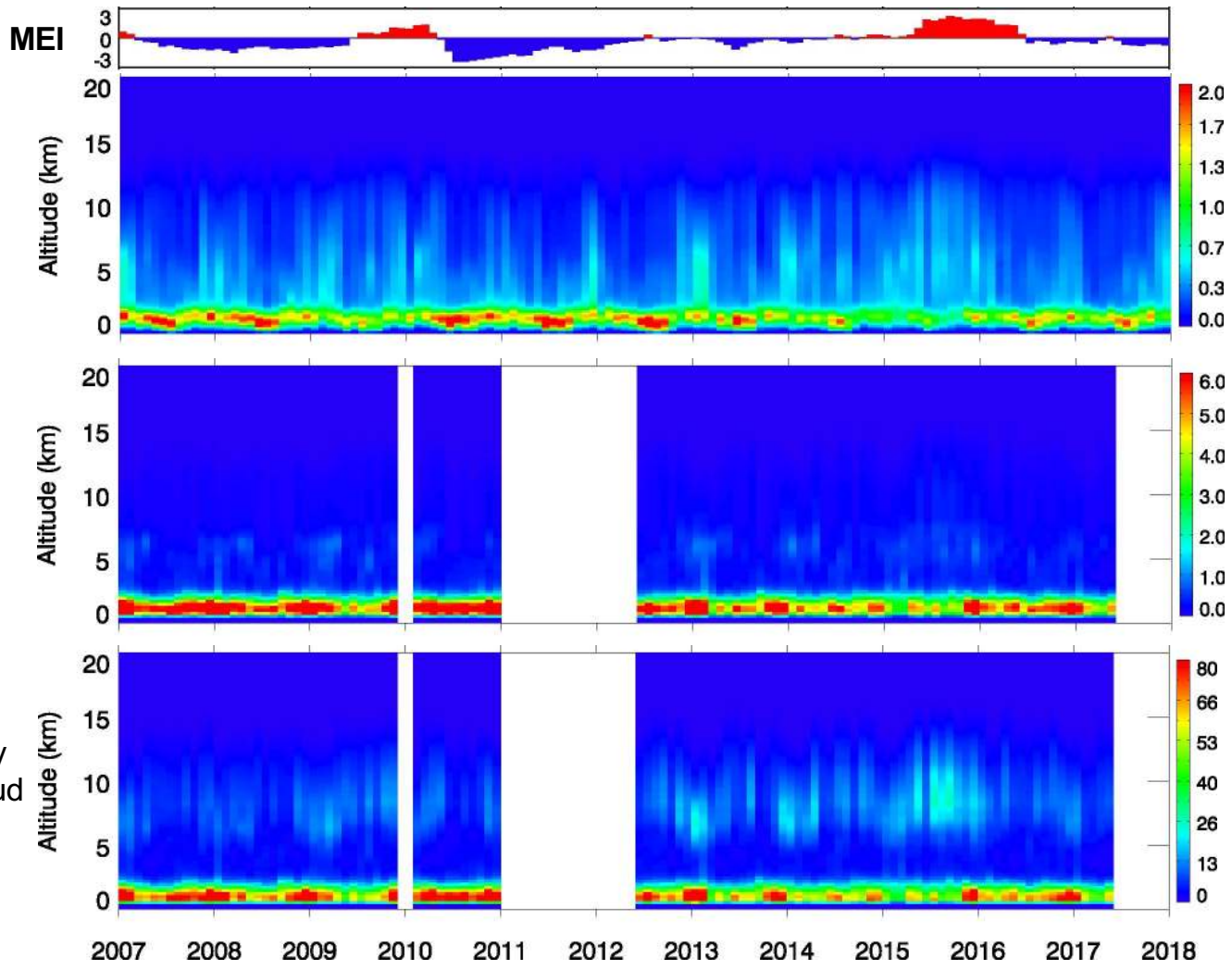

According to MODIS or CloudSat extinction profiles, radiative impacts of high-level clouds are much smaller than those of low-level clouds.

A Closer Look of Cloud Volume Fraction (%) near Surface over the EP (150W-120W, EQ-30N)

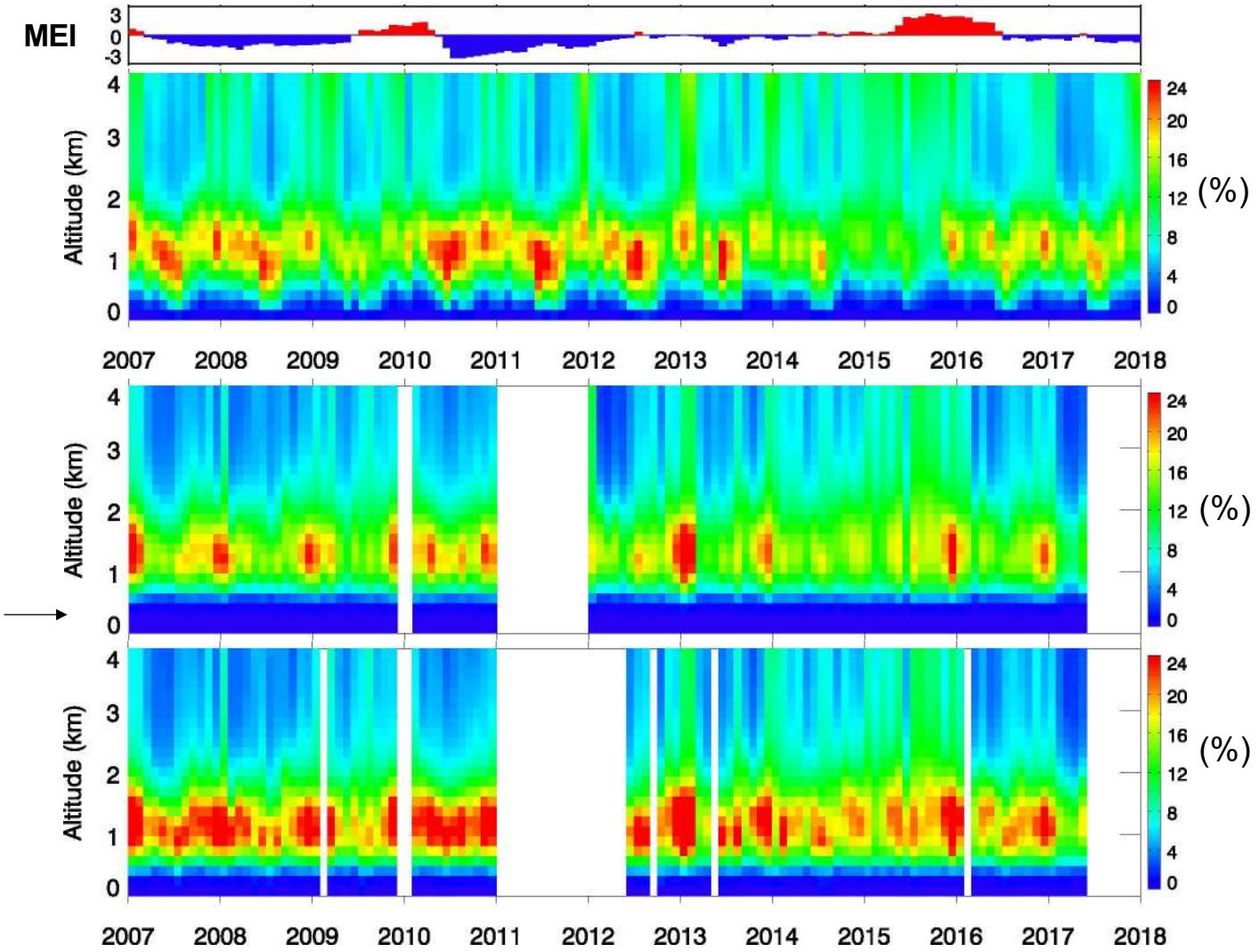

Surface clutters hamper detection of low clouds below 500~ 800 m.

Meteorological conditions over the EP (150W-120W, EQ-30N)

- During El Niño seasons (e.g., the end of 2009 and 2015), positive anomalies in SST, low-troposphere specific humidity, and upward vertical motion occur.
- After positive anomalies of SST, mid/upper troposphere (5-13 km) air temperature increased and tropopause temperature (13-18 km) decreased in the following spring.
- As a result, relative humidity decreased at 5-13 km, and increased at 13-18 km in the next spring of El Niño.

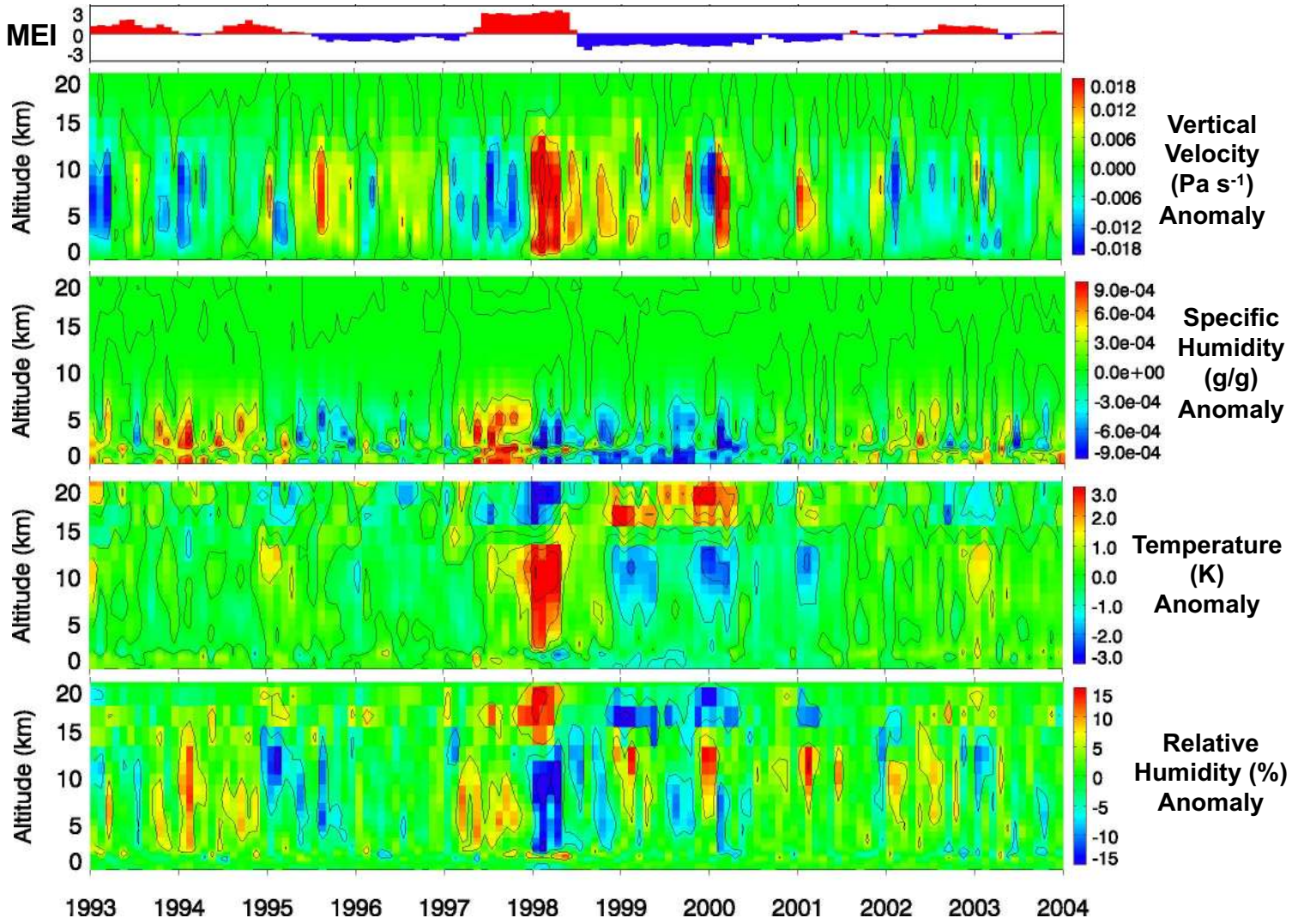

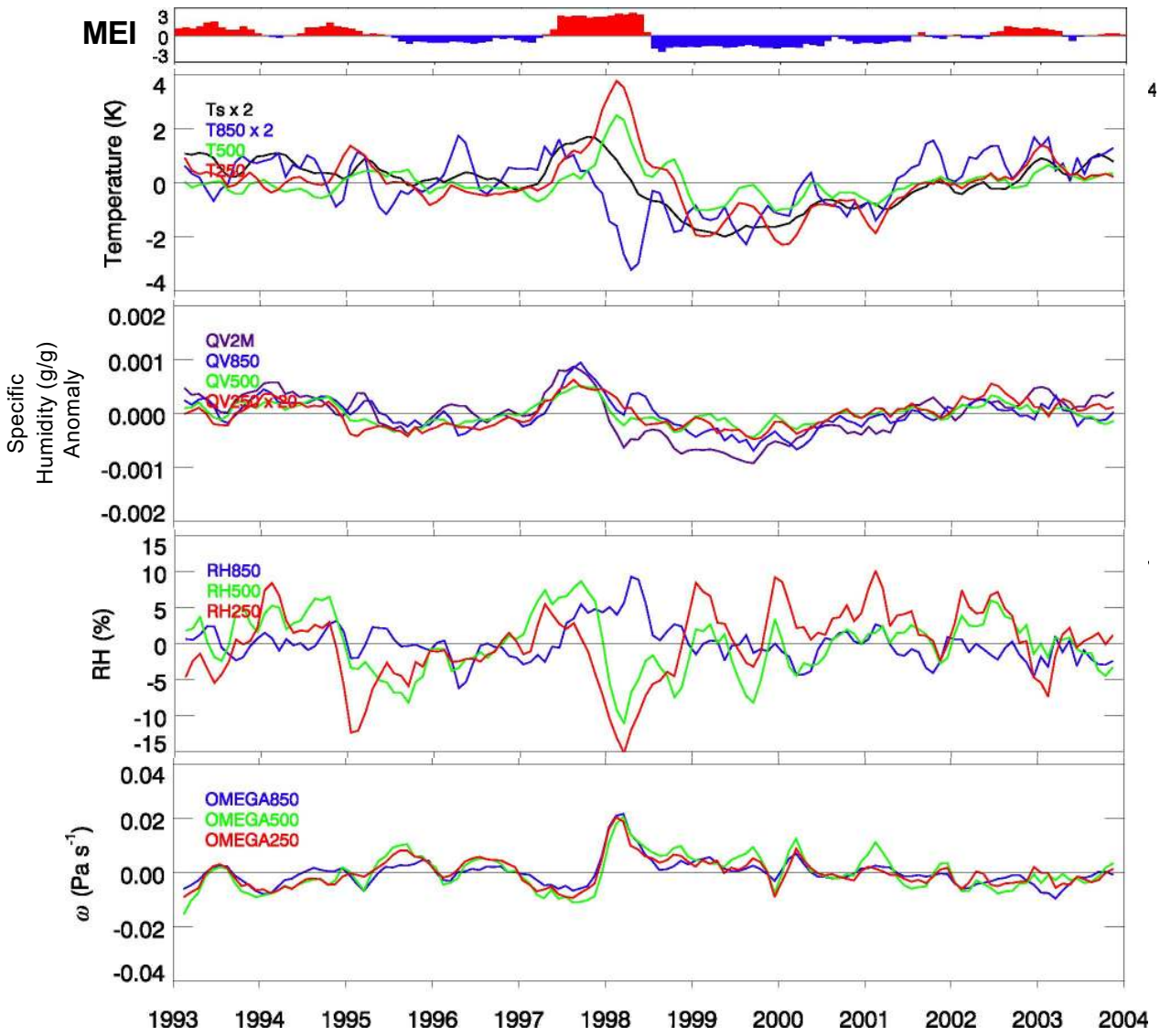
MEI
3
0
-3
Temperature (K)
Ts x 2
T850 x 2
T500
T250
4
2
0
-2
-4
Specific Humidity (g/g) Anomaly
QV2M
QV850
QV500
QV250 x 20
0.002
0.001
0.000
-0.001
-0.002
RH (%)
RH850
RH500
RH250
15
10
5
0
-5
-10
-15
ω (Pa s-1)
OMEGA850
OMEGA500
OMEGA250
0.04
0.02
0.00
-0.02
-0.04
1993
1994
1995
1996
1997
1998
1999
2000
2001
2002
2003
2004

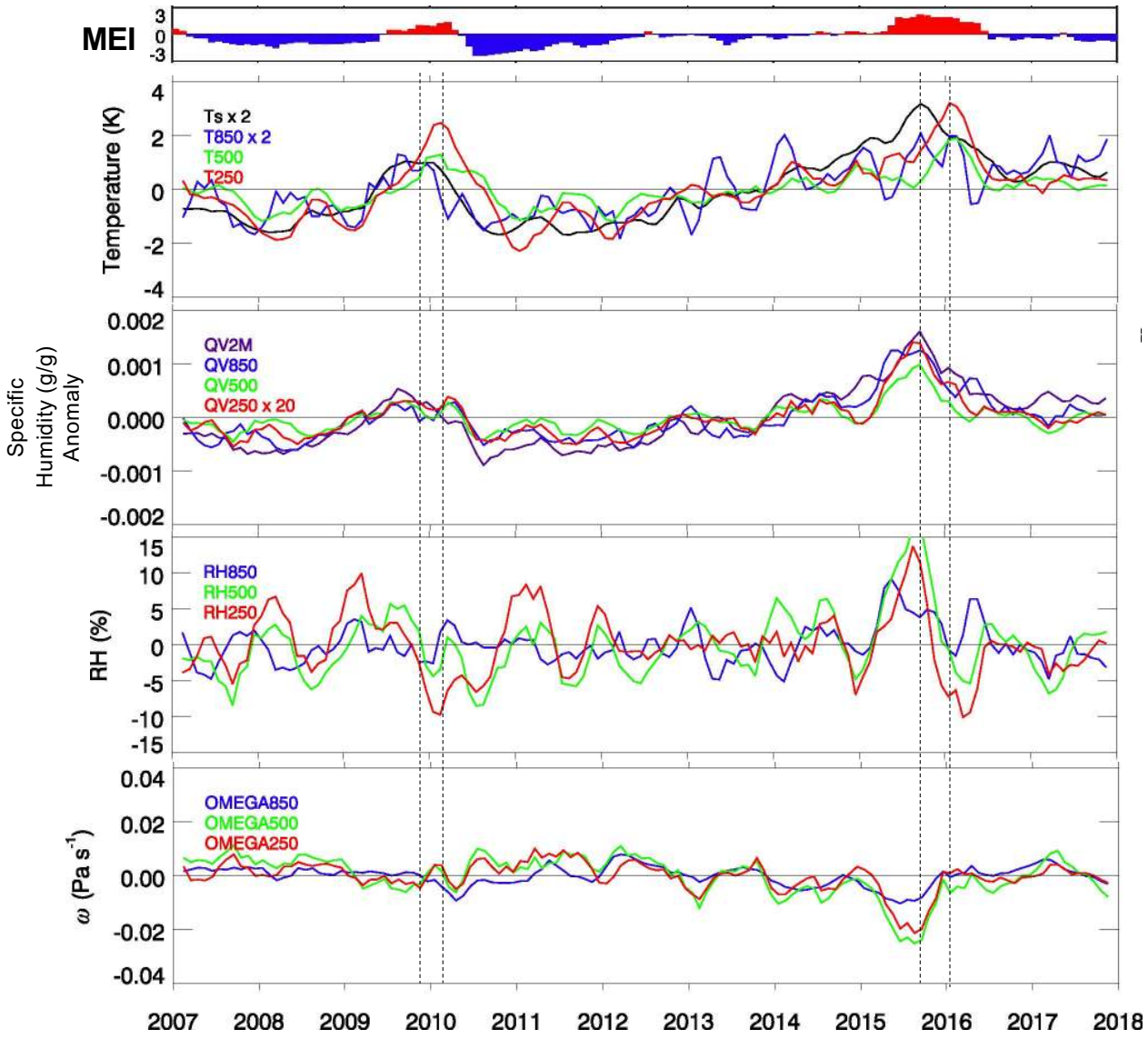
MEI
3
0
-3
Temperature (K)
4
2
0
-2
-4
Ts x 2
T850 x 2
T500
T250
Specific Humidity (g/g) Anomaly
0.002
0.001
0.000
-0.001
-0.002
QV2M
QV850
QV500
QV250 x 20
RH (%)
15
10
5
0
-5
-10
-15
RH850
RH500
RH250
ω (Pa s-1)
0.04
0.02
0.00
-0.02
-0.04
OMEGA850
OMEGA500
OMEGA250
2007
2008
2009
2010
2011
2012
2013
2014
2015
2016
2017
2018

Temperature Response

Radiation R_A

Latent and sensible heat $L(P+C)+F_{sh}$

Advection

$$\frac{1}{g}\nabla_p \cdot \int_0^{p_s} \mathbb{U}(c_pT + \Phi_s + k)dp$$

$$\frac{1}{g}\frac{\partial}{\partial t}\int_0^{p_s}(c_pT + \Phi_s + k)\,dp$$

Total Forcing

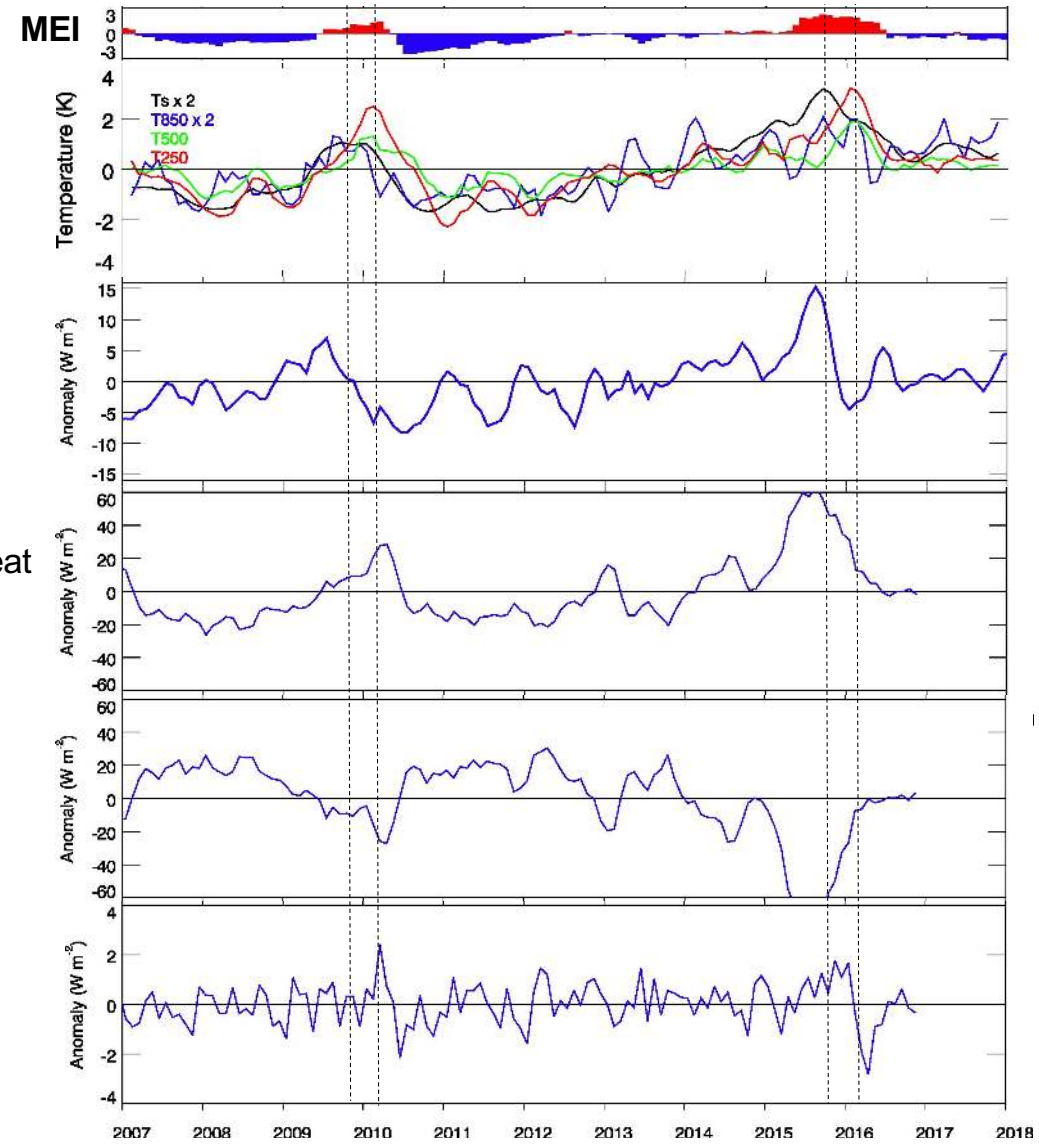

$$\frac{1}{g}\frac{\partial}{\partial t}\int_0^{p_s}(c_pT + \Phi_s + k)\,dp = ADV + (R_A) + L(P+C) + F_{sh}$$

Smoothed with a 3-month moving window

Temperature Response

R_A

$L(P+C)+F_{sh}$

ADV

$\frac{1}{g}\nabla_p \cdot \int_0^{p_s} \mathbb{U}(c_pT + \Phi_s + k)dp$

$\frac{1}{g}\frac{\partial}{\partial t}\int_0^{p_s}(c_pT + \Phi_s + k)\,dp$

Total Forcing

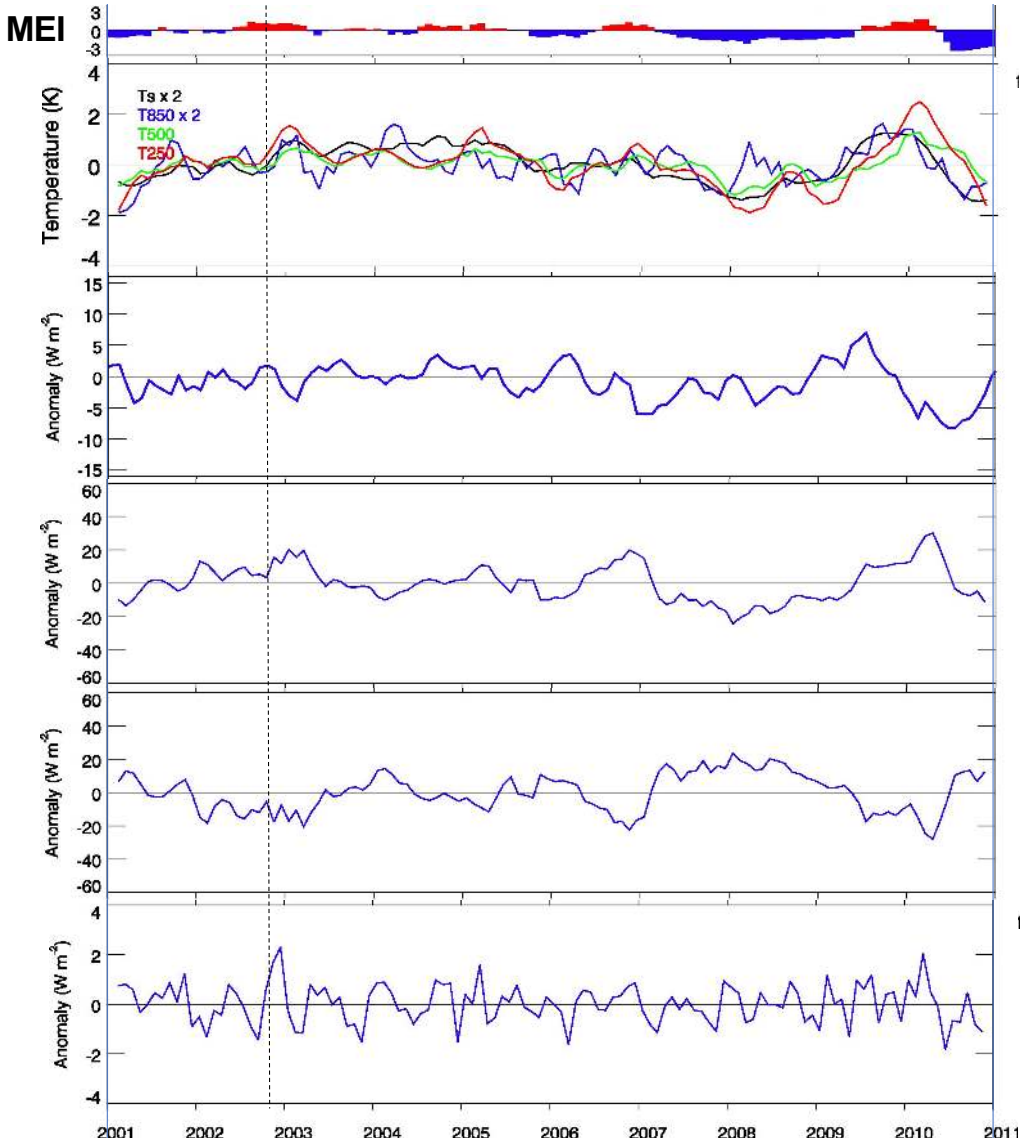

$$\frac{1}{g}\frac{\partial}{\partial t}\int_0^{p_s}(c_pT + \Phi_s + k)\,dp = ADV + (R_A) + L(P+C) + F_{sh}$$

Smoothed with a 3-month moving window